Carbohydrate Polymers 95 (2013) 299–302

Contents lists available at SciVerse ScienceDirect

Carbohydrate Polymers

journal homepage: www.elsevier.com/locate/carbpol

Short communication

Oxygen barrier of multilayer thin films comprised of polysaccharides and clay

Galina Laufer, Christopher Kirkland, Amanda A. Cain, Jaime C. Grunlan*

Department of Mechanical Engineering, Texas A&M University, College Station, TX 77843, United States

ARTICLE INFO

Article history:
Received 5 December 2012
Received in revised form 24 January 2013
Accepted 26 February 2013
Available online 5 March 2013

Keywords:
Layer-by-layer assembly
Renewable materials
Oxygen barrier
Clay
Polysaccharides

ABSTRACT

Multilayered thin films of chitosan (CH), carrageenan (CR) and montmorillonite (MMT) clay, deposited using the layer-by-layer technique, were studied in an effort to produce fully renewable polysaccharide-based thin films with low oxygen permeability. Ten 'trilayers' of CH/MMT/CR (<40 nm thick) on PET film reduced its oxygen permeability (1.76×10^{-15} cm^3 cm/cm^2 s Pa) by an order of magnitude under dry conditions. By adding an additional layer of CH to the trilayer sequence, a 'quadlayer' film of CH/CR/CH/MMT (<60 nm thick) was created, which was able to reduce oxygen permeability of PET by two orders of magnitude under the same conditions. This high oxygen barrier is believed to be due to the unique nanostructure of these films, often referred to as a "nanobrick wall" structure, as well as a strong association amongst the oppositely charged polysaccharides. Combining fully renewable and food contact approved ingredients with high gas barrier and optical transparency makes this technology promising as a foil replacement for food packaging.

1. Introduction

Recently, much attention has been devoted to using bio-based materials as an alternative to man-made polymers for food packaging applications (Bastioli, 2001; Davis & Song, 2006; Eichhorn & Gandini, 2010). Amongst these materials are chitosan and carrageenan, both of which are nontoxic, biodegradable and exhibit antimicrobial properties (Choi et al., 2005; Rabea, Badawy, Stevens, Smagghe, & Steurbaut, 2003). These polysaccharides already have wide application in the food industry (Bixler, 1996; Hambleton, Fabra, Debeaufort, Dury-Brun, & Voilley, 2009) (Lee, Lim, Chong, & Shim, 2009) because they are Generally Recognized as Safe by the U.S. Food and Drug Administration (FDA) (CFR 172.620; GRN No. 170). Carrageenan (CR), which is an anionic sulfated polysaccharide extracted from red seaweeds (McHugh, 1987), and cationic chitosan (CH) extracted from the shells of crustaceans (El-Tahlawy & Hudson, 2006), have already been shown to have oxygen barrier properties (Gallstedt & Hedenqvist, 2002; Hambleton, Debeaufort, Beney, Karbowiak, & Voilley, 2008), but this barrier can be further improved by incorporating montmorillonite (MMT) clay. MMT has been widely studied as an additive to reduce the gas permeability of various polymers (Priolo, Gamboa, & Grunlan, 2010; Triantafyllidis, LeBaron, Park, & Pinnavaia, 2006).

In this study, coatings of renewable food contact approved materials (i.e., chitosan, carrageenan and clay) on PET with varying clay spacing, achieved through layer-by-layer (LbL) deposition, are evaluated for their oxygen permeability at 23 °C and 0% RH. Thickness as well as oxygen barrier of these thin film assemblies can be tailored by altering spacing between clay layers. A film consisting of ten trilayers of CH/MMT/CR reduced oxygen permeability of PET film by an order of magnitude, at a thickness of only 35 nm. Alternately, thicker films (~55 nm) with a quadlayer structure (i.e., CH/CR/CH/MMT) showed greater barrier by reducing oxygen permeability of PET by two orders of magnitude. This relatively simple technology, using renewable ingredients, may be of use for a variety of food packaging applications.

2. Experimental

2.1. Materials

Chitosan (Aldrich, Milwaukee, WI) (MW 50–190 kDa, 75–85% deacetylated) was dissolved in deionized water (18.2 MΩ) to create a 0.2 wt% solution. The pH of this solution was increased to 6 with 1 M sodium hydroxide (NaOH). λ-Carrageenan (Aldrich) was used as a 0.1 wt% solution in deionized water. The pH of this solution was adjusted to 3 with HCl. Sodium montmorillonite clay (tradename Cloisite® Na$^+$, Southern Clay Products, Inc., Gonzales, TX) suspensions were prepared at 1.0 wt% in deionized water. Single-side-polished (1 0 0) silicon wafers (University Wafer, South Boston, MA) were used as the substrate for film thickness

---

* Corresponding author. Tel.: +1 979 845 3027; fax: +1 979 862 3989.
E-mail address: jgrunlan@tamu.edu (J.C. Grunlan).

0144-8617/$ – see front matter © 2013 Elsevier Ltd. All rights reserved.
http://dx.doi.org/10.1016/j.carbpol.2013.02.048

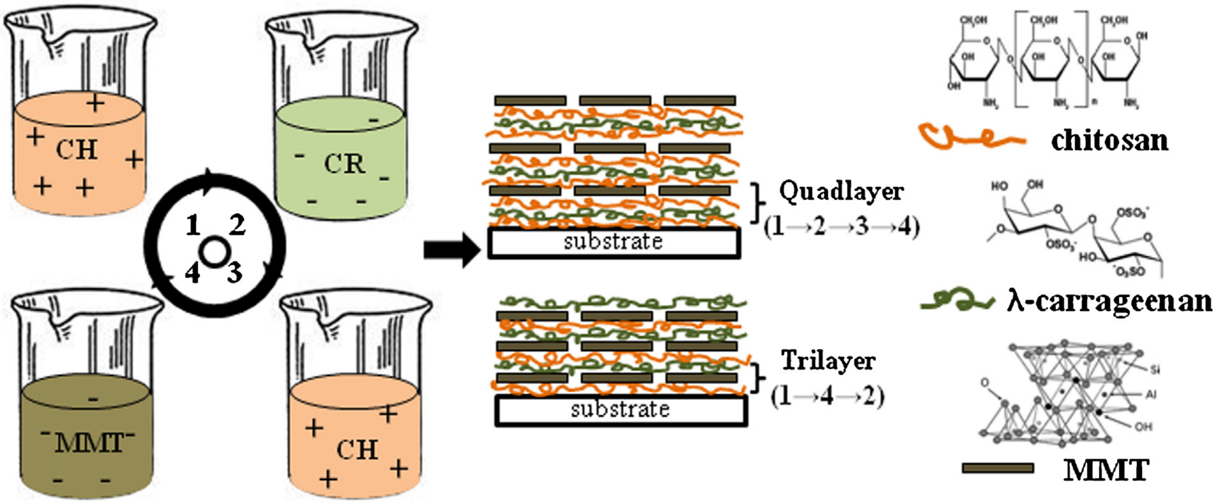

Fig. 1. Schematic of layer-by-layer assembly of renewable materials resulting in thin films with different clay spacing.

characterization and 179 μm thick poly(ethylene terephthalate) film (trade name ST505, produced by Dupont-Teijin), purchased from Tekra (New Berlin, WI), was used for oxygen barrier testing.

2.2. Film preparation

Prior to deposition, plastic substrates were corona treated with a BD-20C Corona Treater (Electro-Technic Products, Inc., Chicago) to create a negative surface charge. All films were deposited on a given substrate using the procedure shown schematically in Fig. 1. Substrates were alternately dipped into chitosan (CH), λ-carrageenan (CR) and montmorillonite (MMT). One cycle of CH/MMT/CR is referred as a trilayer (TL) and one cycle of CH/CR/CH/MMT is referred to as a quadlayer (QL). Initial dips for first two layers were 5 min each and subsequent dips were 1 min. Each dip was followed by rinsing with deionized water and drying with air.

2.3. Characterization

Film thickness was measured with an alpha-SE Ellipsometer (J. A. Woollam Co., Inc., Lincoln, NE). The weight per deposited layer was measured with a Maxtek Research Quartz Crystal Microbalance (RQCM) (Infinicon, East Syracuse, NY), with a frequency range of 3.8–6 MHz, in conjunction with 5 MHz quartz crystals. Clay concentration was measured by a Q50 Thermogravimetric Analyzer (TA Instruments, New Castle, DE) by heating 5–10 mg samples up to 1000 °C at a heating rate of 10 °C/min. Cross sections of chitosan-based assemblies were imaged with a JEOL 1200 EX TEM (JEOL Ltd., Tokyo, Japan), operated at 110 kV. Samples were prepared for imaging by embedding a piece of PET supporting the LbL film in epoxy and sectioning it with a microtome equipped with a diamond knife. Film absorbance was monitored at wavelengths between 190 and 900 nm using a USB2000 UV–vis Spectrometer (Ocean Optics, Dunedin, FL). Oxygen transmission rates were measured by MOCON (Minneapolis, MN) in accordance with ASTM D-3985, using an Oxtran 2/21 ML instrument at 23 °C and 0% RH.

3. Results and discussion

3.1. Film growth and microstructure

Fig. 2 shows the growth of these polysaccharide-based assemblies as a function of the number of cycles (trilayers or quadlayers) deposited. The CH–CR–CH–MMT system exhibits an increased slope around the 4th QL, after which the average thickness increases from 3.5 nm to 5.8 nm for each QL. Interdiffusion of carrageenan could be the origin of this larger growth rate. The exponential growth observed for this system has been observed for a variety of other weak polyelectrolyte systems and its mechanism has been studied in great detail (Picart et al., 2002; Richert et al., 2004). It is unlikely that chitosan would be able to diffuse in and out of the film due to its rigidity (Laufer, Priolo, Kirkland, & Grunlan, 2013; Morris, Castile, Smith, Adams, & Harding, 2009), but CR is more flexible, having been shown to form soft films with weakly charged molecules like poly(allylamine hydrochloride) (Schoeler et al., 2006). CH is weakly charged at pH 6 (pK_a 6–6.5) due to deprotonation of its amine groups (Kurita, 2001). At pH 3, only some of the sulfate groups on the CR molecule are protonated (pK_a ~2), so CH and CR form weakly bonded multilayers (Gu, Decker, & McClements, 2005). Absence of strong bonds between CH and CR enables greater diffusion of CR molecules into the growing film.

No comparable slope change is observed in the trilayer system, consisting of CH/MMT/CR, which grows linearly as a function of cycles deposited. Although CR and MMT are both negatively charged, the successful film build up is possible because hydroxyl groups on carrageenan can form hydrogen bonds with the hydroxyl groups and oxygen on MMT. These relatively strong associations reduce the mobility of CR, making it unable to diffuse in and out of the film, resulting in linear growth. This trend was confirmed with quartz crystal microbalance (QCM) measurements. It has been reported that increasing the hydrophilicity of the surface during growth can cause greater weight to be deposited (Martins, Mano, & Alves, 2010). This has been observed for the systems studied here, where the highest weight deposited corresponds to a carrageenan layer. Water entrapment due to the hydrophillic character of CR is believed to be a key contributing factor (Pinheiro et al., 2012). Chitosan is relatively hydrophobic molecule and in this study it is used close to its solubility limit (Qin, Li, Xiao, Zhu, & Du, 2006; Zheng et al., 2009), which reduces water uptake in the adsorbed layer and results in a smaller measured mass (Indest et al., 2008). It is assumed that the mass corresponding to the adsorption of CR includes entrapped water, preventing film composition from being determined by QCM measurements.

In an effort to overcome the challenges associated with QCM, clay concentration was measured using thermogravimetric analysis. 60 TL and 60 QL films that were heated to 1000 °C to burn off all of the polymeric components. Quadlayer and trilayer films were determined to have 33 wt% and 47 wt% clay, respectively. It

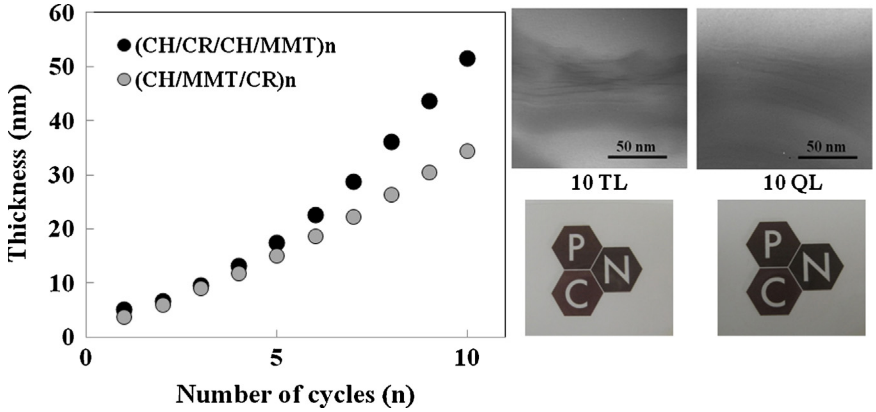

Fig. 2. Film thickness of as a function of cycles deposited (left). TEM cross sections of 10 TL and 10 QL films deposited on PET, with corresponding images of coated PET to highlight film transparency (right).

Table 1
Oxygen permeability of polysaccharide–clay assemblies.

Coating	Permeability ($\times 10^{-16}$ cm^3 cm/cm^2 s Pa)[a]	
	Total (PET + coating)	Coating
Bare PET	17.58	–
10 QL	0.57	0.0003
10 TL	1.92	0.0008
20 BL CH–CR	8.02	0.053
10 BL CH–MMT[b]	N/A	0.0019

[a] 23 °C at 0% RH.
[b] Previously published results (Laufer, Kirkland, et al., 2012).

is nearly impossible to achieve similar clay concentration using traditional processing techniques due to aggregation issues (Gao, 2004). LbL assembly offers precise control of clay platelets orientation, as shown in the TEM cross sections in Fig. 2. In these images, clay platelets can be seen as dark lines with near perfect orientation parallel to the substrate. This "nanobrick wall" structure is also responsible for maintaining excellent optical transparency (Priolo, Gamboa, & Grunlan, 2010). UV–vis spectroscopy reveals that 10 TL and 10 QL films have an average light transmission of 98% across the visible light spectrum (390–750 nm). Images of coated PET films in Fig. 2 highlight this transparency.

3.2. Oxygen barrier properties

The highly oriented nanobrick wall structure described above creates an extremely tortuous path for diffusing oxygen molecules (Laufer, Kirkland, Cain, & Grunlan, 2012; Priolo, Gamboa, Holder, & Grunlan, 2010). Oxygen must bypass impermeable clay platelets by rerouting its path perpendicular to the thickness direction. This results in the low oxygen permeability values shown in Table 1. Although TL and QL films both have 10 layers of clay, their permeability values are quite different. A 10 QL nanocoating (~55 nm thick) reduces the permeability of PET by two orders of magnitude, while the TL counterpart (~35 nm thick) is approximately 2.5× higher. The influence of relative humidity on oxygen barrier is very important for practical applications. It is expected that oxygen permeability will increase with increasing humidity due to swelling of these hydrophilic films, but the barrier effect remains strong (Laufer, Priolo, et al., 2013; Svagan et al., 2012; Yang, Bolling, Priolo, & Grunlan, 2013). The effectiveness if this nanocoating at ambient conditions (22 °C and 55% RH) was demonstrated by depositing 10 TL and 10 QL on bananas that were monitored as a function of time. An uncoated banana turns almost entirely brown by day 9, while coated bananas had just a few brown speckles. As expected, 10 QL looks more effective than 10 TL, as evidenced by smaller and more disparate brown spots (i.e., oxidized skin) (Fig. 3).

This difference in barrier between the TL and QL systems is believed to be due to greater clay spacing in the quadlayers. Increased clay spacing has been previously shown to improve oxygen barrier in LbL thin films (Priolo, Gamboa, & Grunlan, 2010). This effect is more evident when compared to the previously studied CH–MMT bilayer system (Laufer, Kirkland, et al., 2012). To eliminate the substrate effect (CH/MMT was tested on PLA) coating permeability was decoupled from the substrate using a previously described method (Roberts et al., 2002). An extra CR layer improves the CH/MMT system by a factor of more than two, from 1.9×10^{-19} cm^3 cm/cm^2 s Pa to 8×10^{-20} cm^3 cm/cm^2 s Pa. Besides increase in clay spacing, another possible reason for the improved barrier of the TL and QL systems is the interaction between the oppositely charged functional groups of CH and CR, which results in a more tightly packed layer. This hypothesis was confirmed by testing 20 BL coating consisting of CH and CR alone, which cut the permeability of PET in half, largely due to the interpenetrating

Fig. 3. Comparison of ripeness as function of time (from left to right) between uncoated control and bananas coated with 10 TL and 10 QL assemblies. Bananas were aged under ambient conditions (22 °C and 55% RH).

structure (i.e., reduced free volume) of these two polysaccharides. A similar situation was previously observed with non-renewable polyethylenimine and poly(acrylic acid) (Yang, Haile, Park, Malek, & Grunlan, 2011).

4. Conclusions

Nanocoatings made with renewable chitosan, carrageenan and montmorillonite clay were deposited on PET film using layer-by-layer assembly. Visible light transmission data revealed that these films were greater than 98% transparent due to highly orientated and exfoliated clay platelets that was confirmed by TEM imaging. Oxygen barrier was shown to improve with greater spacing between clay layers. The 55 nm thick, 10 QL film (CH/CR/CH/MMT) reduced the oxygen permeability of PET by two orders of magnitude. The ability to produce thin films with such high oxygen barrier and optical transparency, with a relatively small number of layers and GRAS materials, provides an opportunity for a renewable foil replacement for food packaging. There are likely other renewable polyelectrolytes (e.g., alginate, carboxymethylcellulose, and lignin) that could further improve the barrier shown here and this is the focus of ongoing work.

References

Bastioli, C. (2001). Globas status of the production of biobased packaging materials. *Starch*, *53*(8), 351–355.

Bixler, H. J. (1996). Recent developments in manufacturing and marketing carrageenan. *Hydrobiologia*, *327*, 35–57.

CFR 172.620. U. S. Food and Drug Administration: Generally Recognized as Safe.

Choi, J. H., Choi, W. Y., Cha, D. S., Chinnan, M. J., Park, H. J., Lee, D. S., et al. (2005). Diffusivity of potassium sorbate in κ-carrageenan based antimicrobial film. *LWT-Food Science and Technology*, *38*(4), 417–423.

Davis, G., & Song, J. H. (2006). Biodegradable packaging based on raw materials from crops and their impact on waste management. *Industrial Crop and Products*, *23*(2), 147–161.

Eichhorn, S. J., & Gandini, A. (2010). Materials from renewable resources. *MRS Bulletin*, *35*(3), 187–190.

El-Tahlawy, K., & Hudson, S. M. (2006). Chitosan: Aspects of fiber spinnability. *Journal of Applied Polymer Science*, *100*, 1162–1168.

Gallstedt, M., & Hedenqvist, M. S. (2002). Oxygen and water barrier properties of coated whey protein and chitosan films. *Journal of Polymers and the Environment*, *10*(1-2), 1–4.

Gao, F. (2004). Clay/polymer composites: The story. *Materials Today*, *7*(11), 50–55.

GRN No. 170. US Food and Drug Administration: GRAS Notices.

Gu, Y. S., Decker, E. A., & McClements, D. J. (2005). Influence of pH and carrageenan type on properties of β-lactoglobulin stabilized oil-in-water emulsions. *Food Hydrocolloids*, *19*(1), 83–91.

Hambleton, A., Debeaufort, F., Beney, L., Karbowiak, T., & Voilley, A. (2008). Protection of active aroma, compound against moisture and oxygen by encapsulation in biopolymeric emulsion-based edible films. *Biomacromolecules*, *9*(3), 1058–1063.

Hambleton, A., Fabra, M.-J., Debeaufort, F., Dury-Brun, C., & Voilley, A. (2009). Interface and aroma barrier properties of iota-carrageenan emulsion-based films used for encapsulation of active food compounds. *Journal of Food Engineering*, *93*(1), 80–88.

Indest, T., Laine, J., Ribitsch, V., Johansson, L.-S., Stana-Kleinschek, K., & Strnad, S. (2008). Adsorption of chitosan on PET films monitored by quartz crystal microbalance. *Biomacromolecules*, *9*(8), 2207–2214.

Kurita, K. (2001). Controlled functionalization of the polysaccharide chitin. *Progress in Polymer Science*, *26*(9), 1921–1971.

Laufer, G., Kirkland, C., Cain, a. A., & Grunlan, J. C. (2012). Clay–chitosan nanobrick walls: Completely renewable gas barrier and flame-retardant nanocoatings. *ACS Applied Materials and Interfaces*, *4*(3), 1643–1649.

Laufer, G., Priolo, M. A., Kirkland, C., & Grunlan, J. (2013). High oxygen barrier, clay and chitosan-based multilayer thin films: An environmentally-friendly foil replacement. *Green Materials*, *1*(1), 4–10.

Lee, D. W., Lim, H., Chong, H. N., & Shim, W. S. (2009). Advances in chitosan material and its hybrid derivatives: A review. *The Open Biomaterials Journal*, *1*, 10–20.

Martins, G. V., Mano, J. F., & Alves, N. M. (2010). Nanostructured self-assembled films containing chitosan fabricated at neutral pH. *Carbohydrate Polymers*, *80*(2), 570–573.

McHugh, D. J. (1987). Production, properties and uses of carrageenan. In *Production and utilization of products from commercial seaweeds*. Rome, Italy: Food and Agriculture Organization of the United Nations.

Morris, G. A., Castile, J., Smith, A., Adams, G. G., & Harding, S. E. (2009). Macromolecular conformation of chitosan in dilute solution: A new global hydrodynamic approach. *Carbohydrate Polymers*, *76*, 616–621.

Picart, C., Mutterer, J., Richert, L., Luo, Y., Prestwich, G. D., Schaaf, P., et al. (2002). Molecular basis for the explanation of the exponential growth of polyelectrolyte multilayers. *Proceedings of the National Academy of Sciences of the United States of America*, *99*(20), 12531–12535.

Pinheiro, A. C., Bourbon, A. I., Medeiros, B. G., da Silva, L. H. M., da Silva, M. C. H., Garneiro-da-Cunha, M. G., et al. (2012). Interactions between κ-carrageenan and chitosan in nanolayered coatings – Structural and transport properties. *Carbohydrate Polymers*, *87*(2), 1081–1090.

Priolo, M., Gamboa, D., & Grunlan, J. C. (2010). Transparent clay-polymer nano brick wall assemblies with tailorable oxygen barrier. *ACS Applied Materials and Interfaces*, *2*, 312.

Priolo, M., Gamboa, D., Holder, K., & Grunlan, J. C. (2010). Super gas barrier transparent polymer-clay multilayer ultrathin film. *Nano Letters*, *10*(12), 4970–4974.

Qin, C., Li, H., Xiao, Q., Zhu, J., & Du, Y. (2006). Water-solubility of chitosan and its antimicrobial activity. *Carbohydrate Polymers*, *63*(3), 367–374.

Rabea, E. I., Badawy, M. E., Stevens, C. V., Smagghe, G., & Steurbaut, W. (2003). Chitosan as intimicrobial agent: Applications and mode of action. *Biomacromolecules*, *4*(6), 1457–1465.

Richert, L., Lavalle, P., Payan, E., Shu, X. Z., Prestwich, G. D., Stoltz, J. F., et al. (2004). Layer-by-layer buildup of polysaccharide films: Physical chemistry and cellular adhesion aspects. *Langmuir*, *20*(2), 448–458. http://dx.doi.org/10.1021/La035415n

Roberts, A. P., Henry, B. M., Sutton, A. P., Grovenor, C. R. M., Briggs, G. A. D., Miyamoto, T., et al. (2002). Gas permeation in silicon-oxide/polymer (SiOx/PET) barrier films: Role of the oxide lattice, nano-defects and macro-defects. *Journal of Membrane Science*, *208*(1-2), 75–88.

Schoeler, B., Delorme, F., Doench, I., Sukhorukov, G., Fery, A., & Glinel, K. (2006). Polyelectrolyte films based on polysaccharides of different conformations: Effects on multilayer structure and mechanical properties. *Biomacromolecules*, *7*(6), 2065–2071.

Svagan, A. J., Akesson, A., Cardenas, M., Bulut, S., Knudsen, J. C., Risbo, J., et al. (2012). Transparent films based on PLA and montmorillonite with tunable oxygen barrier properties. *Biomacromolecules*, *13*(2), 397–405.

Triantafyllidis, K. S., LeBaron, P. C., Park, I., & Pinnavaia, T. J. (2006). Epoxy-clay fabric film composites with unprecedented oxygen-barrier properties. *Chemistry of Materials*, *18*(18), 4393–4398.

Yang, Y.-H., Bolling, L., Priolo, M. A., & Grunlan, J. C. (2013). Super gas barrier and selectivity of graphene oxide-polymer multilayer thin films. *Advanced Materials*, *25*(4), 503–508.

Yang, Y.-H., Haile, M., Park, Y. T., Malek, F. A., & Grunlan, J. C. (2011). Super gas barrier of all-polymer multilayer thin films. *Macromolecules*, *44*(6), 1450–1459.

Zheng, Z. H., Wei, Y. J., Wang, G., Wang, A. J., Ao, Q., Gong, Y. D., et al. (2009). Surface properties of chitosan films modified with polycations and their effects on the behavior of PC12 cells. *Journal of Bioactive and Bompatible Polymers*, *24*(1), 63–82.